Chinese Chemical Letters 34 (2023) 108296

Contents lists available at ScienceDirect

Chinese Chemical Letters

journal homepage: www.elsevier.com/locate/cclet

Chemical proteomic profiling with photoaffinity labeling strategy identifies antimalarial targets of artemisinin

Peng Gao[a,1], Jiayun Chen[a,1], Peng Sun[a,1], Jianyou Wang[b,1], Huan Tang[a,1], Fei Xia[a], Liwei Gu[a], Huimin Zhang[c], Chen Wang[a], Yin Kwan Wong[a], Yinhua Zhu[a], Chengchao Xu[a,*], Jigang Wang[a,c,d,*]

[a] Artemisinin Research Center, and Institute of Chinese Materia Medica, China Academy of Chinese Medical Sciences, Beijing 100700, China
[b] Pharmaceutical College, Henan University, Kaifeng 475004, China
[c] Shandong Academy of Chinese Medicine, Ji'nan 250014, China
[d] Department of Nephrology, Shenzhen Key Laboratory of Kidney Diseases, Shenzhen Clinical Research Centre for Geriatrics, Shenzhen People's Hospital, The First Affiliated Hospital, Southern University of Science and Technology, Shenzhen 518020, China

ARTICLE INFO

Article history:
Received 30 October 2022
Revised 25 February 2023
Accepted 2 March 2023
Available online 5 March 2023

Keywords:
Artemisinin
Antimalarial
Chemical proteomic
Target identification
Photoaffinity probe

ABSTRACT

Present research on the antimalarial mechanisms of artemisinin (ART) is mainly focused on covalent drug binding targets alkylated by free radicals, while non-covalent binding targets have rarely been reported. Here, we developed a novel photoaffinity probe of ART to globally capture and identify the antimalarial target proteins of ART through chemical proteomics. The results demonstrated that ART can bind to parasite proteins by both covalent and non-covalent modification, and these may jointly contribute to the antimalarial effects. Our work enriches the research on the antimalarial targets of ART, and provides a new perspective for further exploring the antimalarial mechanism of ART.

Malaria remains a severe threat to global human health, accounting for 247 million cases and approximately 619,000 deaths in 2021 [1]. Artemisinin (ART), as the recommended first-line drug for malaria treatment, occupies a decisive position in confronting the malaria threat and the spread of multidrug resistance [2]. In the past decades, the mechanism of action of ART has been extensively studied, especially in the background of the emergence of anti-malaria drug resistance [3,4]. In our previous study, we used the activity-based protein profiling (ABPP) strategy to demonstrate for the first time that the unparalleled antimalarial effect of ART is a result of the activation of its peroxide bridge by ferrous heme [5]. Once activated, a variety of parasite proteins and lipids are alkylated by free radicals of ART, forming covalent bonds with the drug and leading to the rapid death of parasites [6,7]. Furthermore, ferrous heme as the activator of ART was also the target of ART alkylation [8,9], which results in the inability to form haemozoin (Hz) and parasite toxicity [10]. Using similar ABPP strategies, numerous studies subsequently identified a series of covalent protein targets of ART using clickable ART-derived probes with alkyne or azide handles [11,12].

Although heme-mediated covalent protein modification has been interpreted as a key mechanism of ART anti-malaria activity, ART may also bind to proteins and DNA in a non-covalent manner in parasites [13–15]. Moreover, mechanistic studies of the other pharmacological activities of ART (including antidiabetic and anticancer activity) have also reported that certain functions of ART are independent of covalent binding reactions by free radical alkylation [16,17]. However, studies of the non-covalent protein targets of ART and their roles in the anti-malaria effects of ART remain scarce. Chemoproteomic profiling of non-covalent targets of ART in malaria parasites would thus provide more comprehensive and in-depth insights into ART's antimalarial mechanism.

In order to comprehensively enrich and identify the target proteins of ART, including both covalent and non-covalent binding proteins, we introduced a photoaffinity labeling strategy based on ABPP in this work [18,19]. First, we designed and synthesized an activity-based ART photoaffinity probe (APP) according to the synthesis scheme in Fig. 1A, where a diazirine photoreactive group and alkyne report handle were incorporated in the carbonyl position without changing the endoperoxide bridge pharmacophore [20]. The diazirine group in APP can react with the nucleophilic

* Corresponding authors.
E-mail addresses: ccxu@icmm.ac.cn (C. Xu), jgwang@icmm.ac.cn (J. Wang).
[1] These authors contributed equally to this work.

https://doi.org/10.1016/j.cclet.2023.108296
1001-8417/

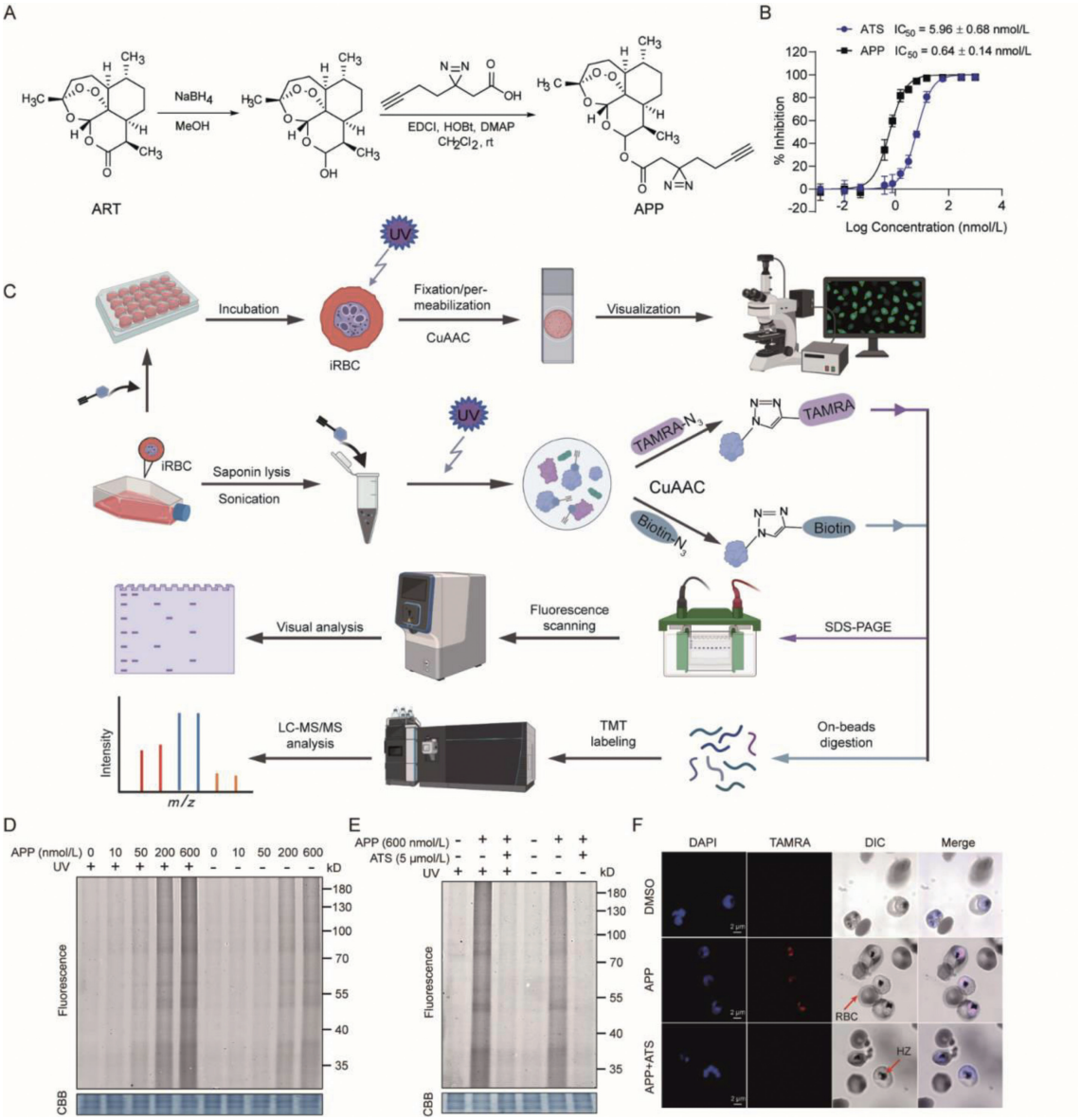

Fig. 1. (A) Synthesis scheme of artemisinin photoaffinity activity probe (APP). (B) Determination of antimalaria activity of APP and artesunate (ATS) against *P. falciparum* 3D7 strain. (C) General workflow of APP-mediated ABPP used to label and identify artemisinin (ART) target proteins. (D) *In vitro* labelling for 4 h of APP in parasite lysate with or without UV irradiation in dose-dependent manner. (E) Excessive ATS can specifically compete the target proteins of APP under and without UV irradiation. (F) Confocal imaging showed that APP (600 nmol/L) could rapidly distribute to the parasites after incubation with infected red blood cells (iRBC) for 1 h, and was eliminated by pre-incubated excess ATS (3 μmol/L) under UV irradiation (Scale bar = 2 μm). HZ, hemozoin; TAMRA, carboxytetramethylrhodamine; CBB, Coomassie brilliant blue.

residues of adjacent proteins by producing carbon free radicals under ultraviolet (UV) irradiation ($\lambda = 365$ nm), which enabled the unbiased identification of non-covalent ART targets [21,22]. We measured and compared the half-maximal inhibitory concentrations (IC_{50}) of APP and artesunate (ATS), which is a commonly used ART derivative with high aqueous solubility and similar parasiticidal ability as ART, against the *Plasmodium falciparum* (*P. falciparum*) 3D7 strain. The IC_{50} values of ATS and APP against 3D7 were 5.96 and 0.64 nmol/L, respectively (Fig. 1B). The outstanding antimalarial activity of APP, which is superior to ATS could also be observed in the *P. falciparum* 7G8 strain (Fig. S1 in Supporting information).

We next used the APP to perform fluorescence labeling experiments with or without UV irradiation according to the workflow represented in Fig. 1C. As depicted in Fig. 1D, the fluorescence intensity of parasite proteins labeled by APP increased in a dose-dependent manner, regardless of the presence of UV irradiation. In addition, the fluorescence intensity of the UV irradiation group was slightly stronger than that of the non-UV irradiation group at the same concentration. This showed that in addition to irreversible covalent binding to proteins through free radical reaction, ART could indeed also bind some proteins reversibly in a non-covalent manner, or bind to the same target protein in both ways. Moreover, ATS could competitively inhibit the fluorescence signals of APP labeling under the two conditions (Fig. 1E), indicating that most of the non-covalent and covalent targets of APP should be the same as those of ATS. To further confirm ART binding to proteins in parasites, we conducted *in vivo* imaging of living cells by APP labeling under UV irradiation. The red fluorescence arising from the APP was observed to rapidly distribute and accumulate in infected red blood cells (RBC) within 30 min, but not in the normal RBCs. Addition of excess ATS could eliminate the red fluorescence from the APP labeling, which was consis-

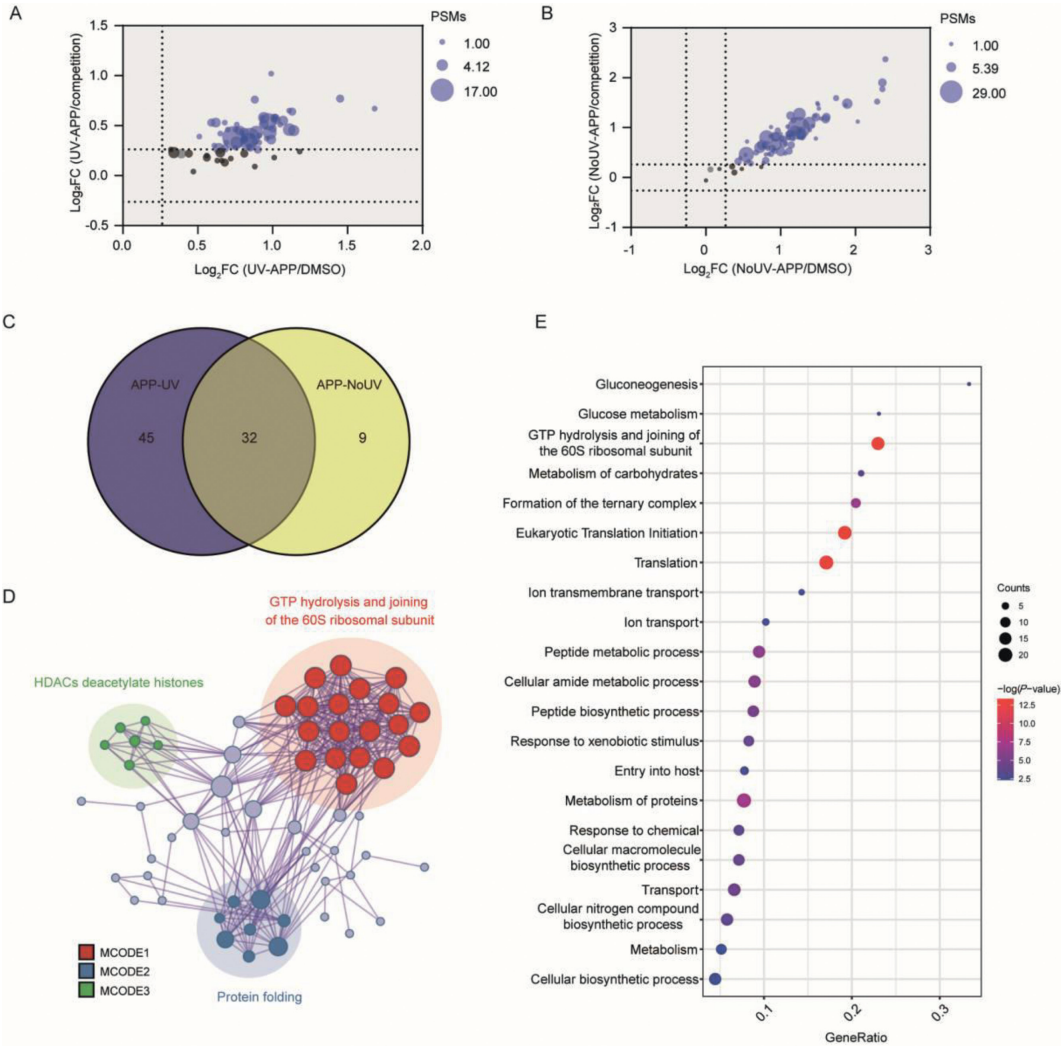

Fig. 2. Scatter plot of 77 (A) and 41 (B) target proteins identified by APP based on ABPP experiments under or without UV irradiation. Both graphs are displayed with the mean $\log_2$ ratio of the relative abundances between APP (600 nmol/L) and DMSO group (*x*-axis) against the APP and competition group (600 nmol/L APP + 3 μmol/L ATS) (*y*-axis). The fold change (FC) > 1.2 and Padj < 0.05 were used as hit selection criteria. The full list of identified target proteins are shown in Tables S1 and S2 in Supporting information. (C) Venn diagram of target proteins identified by APP under the two different conditions. (D) Protein–protein interaction (PPI) networks of all 86 identified target proteins. (E) Gene ontology (GO) analysis of the enriched biological process (BP) for 86 identified target proteins by APP-based ABPP.

tent with the fluorescent labeling in gel (Fig. 1F) [23]. Collectively, we showed here that APP is a novel and satisfactory photoaffinity probe with similar activity to ATS, and can be further used to profile the non-covalent and covalent targets of ART by chemical proteomics.

As the fluorescence labeling results showed that ATS could bind both reversibly and irreversibly to parasite proteins, we next identified and distinguished the protein targets of APP in the UV irradiation and non-UV irradiation treatment groups by the chemical proteomics approach. The protein targets labelled by the alkyne-tagged APP were first linked with biotin-azide tags *via* copper catalyzed azide alkyne cycloaddition (CuAAC), then pulled down by streptavidin beads. The enriched proteins were then identified and quantified by liquid chromatography-tandem mass spectrometry (LC-MS/MS) combined with tandem mass tags (TMT) labeling (Fig. 1C). There were 77 and 41 protein targets identified from the UV irradiation and non-UV irradiation groups respectively (Figs. 2A and B), of which 32 proteins were overlapped for a total of 86 unique proteins (Fig. 2C). The overlapped targets indicated proteins that could interact with ART by both covalent and non-covalent binding modes. More importantly, 45 proteins were identified only in the UV irradiation group, indicating that these proteins were likely to bind to ART in a mainly non-covalent manner. The above results demonstrated that during the accumulation process in parasites, there was covalent binding between proteins and activated ART, but also existing non-covalent binding interactions simultaneously [23]. However, the non-covalent interactions of these targets with ART may have been missed by previous studies which did not employ photoaffinity probes.

Confirming the presence of non-covalent interactions strengthened our belief that a holistic identification of ART targets (including novel non-covalent targets) may provide more comprehensive insights into the antimalaria mechanisms of ART compared to previous studies. We then carried out a bioinformatics analysis of the 86 unique protein targets. The protein–protein interaction (PPI) analysis revealed the interaction networks focused on guanosine triphosphate (GTP) hydrolysis, histone deacetylases (HDACs) deacetylate histones and protein folding (Fig. 2D). Furthermore, the gene ontology (GO) analysis showed that the pathway of glucose production and metabolism was highly enriched (Fig. 2E). Therefore, the glucose metabolism-related pathway may be a key pathway by which ART kills the parasite.

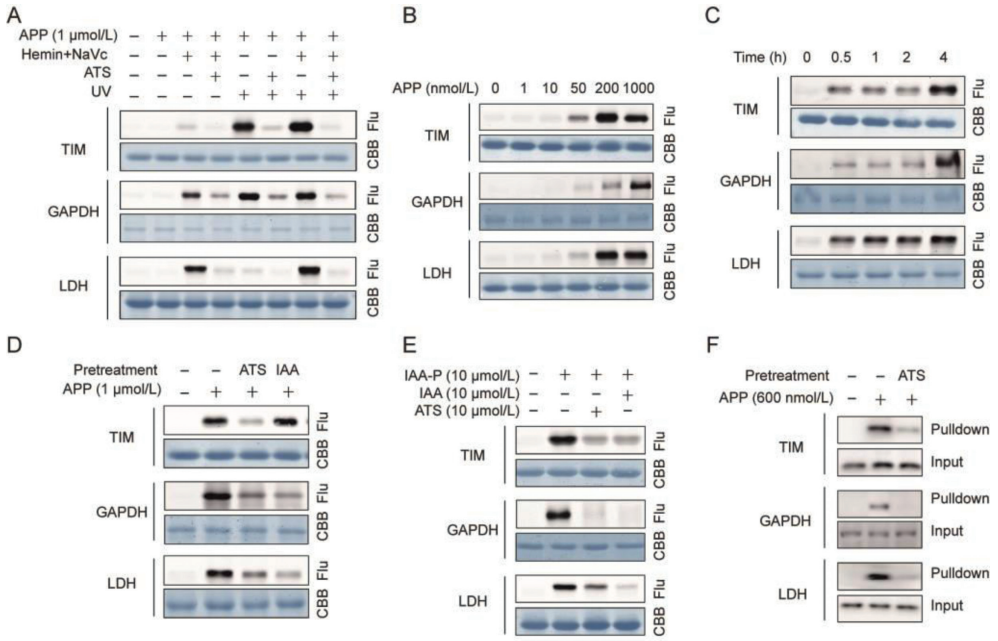

Fig. 3. (A) Fluorescence labeling of recombinant *Pf*TIM, *Pf*GAPDH, *Pf*LDH proteins with APP. (B) APP (1 μmol/L) activated with heme (hemin+NaVc) specifically binds to recombinant proteins in dose-dependent and (C) time-dependent manners under UV irradiation. (D) Pre-incubation with excess ATS (10 μmol/L) and IAA (10 μmol/L) can compete with APP binding to recombinant proteins. (E) ATS can compete for the binding of IAA-P to recombinant proteins. (F) Validation of the specific binding of APP to the 3 target proteins *in situ* by pull-down Western blot. Flu, fluorescence.

In the erythrocyte stage of *P. falciparum*, parasite survival heavily relies on the energy provided by anaerobic glycolysis for its rapid metabolism [24]. The glucose consumption level of parasites is 30–50 folds higher than the host cell [25], due to the higher activity and expression of the relevant metabolic enzymes, which may be natural targets for antimalarial drugs [26,27]. Three enzymes in the glucose glycolysis pathway, L-lactate dehydrogenase (*Pf*LDH, *PF3D7_1324900*), triosephosphate isomerase (*Pf*TIM, *PF3D7_1439900*) and glyceraldehyde-3-phosphate dehydrogenase (*Pf*GAPDH, *PF3D7_1462800*) were found in our target database. LDH participates in the last step of glycolysis by catalyzing the conversion of pyruvate to lactic acid [25]. TIM is a dimeric glycolytic enzyme, which catalyses the isomerization of D-glyceraldehyde-3-phosphate to dihydroxyacetone phosphate and plays an important role in gluconeogenesis [28]. A previous study has shown that during malaria infection, patients can develop severe hemolytic anemia because of the antibody response to TIM [29]. GAPDH reduces glyceraldehyde-3-phosphate to 1,3-bisphosphoglycerate [30], and inhibition of GAPDH can prevent the production of ATP and accelerate the consumption of ATP. Moreover, GAPDH has been regarded as a potential biomarker for malaria diagnosis [31,32].

Next, we successfully expressed and purified the recombinant proteins of the three glycolysis-related enzymes to validate their interactions with ART. First, their binding behaviours with APP under different conditions were evaluated by fluorescence labeling (Fig. 3A). Under UV irradiation, the labeling intensity of TIM by APP was significantly higher than that under click chemistry conditions with the addition of hemin and sodium ascorbate (NaVc), suggesting that TIM is an ART target of mainly relying on non-covalent binding interaction. In contrast, LDH is likely a covalent target of ART based on the reversed result in the labeling intensity under the same conditions. As for GAPDH, similar labeling effects under the two conditions indicates that it is both a covalent and non-covalent target of ART. In addition, the labeling intensity of the three enzymes by APP was both dose-dependent (Fig. 3B) and time-dependent (Fig. 3C), and could be eliminated by pre-incubation of ATS (Fig. 3D). Similar competitive effects were also observed in the *in situ* pull-down Western-blot experiments (Fig. 3F). Interestingly, after pre-incubation with the cysteine (Cys) residue blocker Iodoacetamide (IAA), the fluorescence labeling intensity of APP was weakened by varying degrees (Fig. 3D), while the fluorescence labeling of protein by IAA-alkynyl probe (IAA-P) was almost completely eliminated after pre-treatment of proteins with ATS (Fig. 3E), suggesting that Cys may be one of the sites of ATS binding to the targets.

Moreover, we confirmed high co-localization of APP with its protein targets, as well as with mitochondria (the primary site of glucose metabolism) through immunofluorescence experiments (Figs. 4A and B). More importantly, enzyme activity experiments showed that ATS could efficaciously inhibit the catalytic activity of the identified targets in a dose-dependent manner (Figs. 4D–F). Based on these evidences, we conclude that ART could directly bind key enzymes related with glucose metabolism *via* covalent or non-covalent binding modes, and further inhibit their activity, which finally leads to parasite death by hampering the energy metabolism process. Subsequently, to identify the possible covalent binding sites of ART binding to the proteins of interest, we used tandem mass spectrometry to precisely locate the binding residues in *Pf*LDH after ATS incubation, identifying valine 53 (Val 53) as the binding site which was further validated by Docking simulation (Figs. 4C and G).

In conclusion, we explored the target proteins and binding modes of ART in parasites by developing a photoaffinity probe of ART, and verified these results in a subset of proteins. The results showed that ART can bind to parasite proteins by both covalent and non-covalent modification, and these might jointly contribute to the antimalarial effect. However, the relationship between the two binding modes in the antimalarial process still need to be further explored. Our work enriches the research on the antimalarial targets of ART, and provides a new perspective for further exploring the antimalarial mechanism of ART.

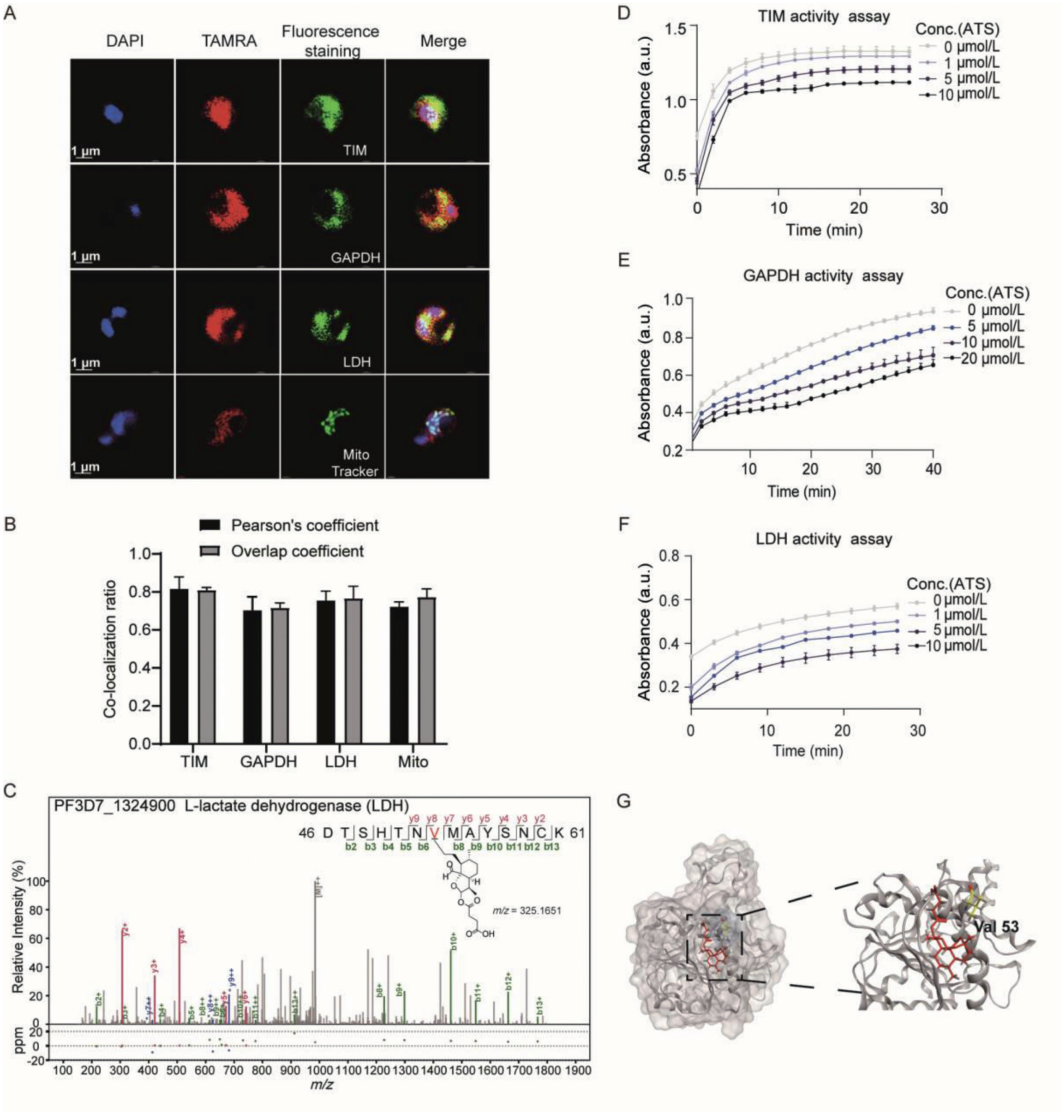

Fig. 4. (A) Immunofluorescence co-localization of APP with target proteins and mitochondria by immunofluorescence experiment under UV irradiation. Scale bar: 1 μm. (B) Quantitative analysis of co-localization with Pearson's coefficient and Overlap coefficient. (C) Identification of the binding site of ATS on the recombinant *Pf*LDH protein. (D–F) ATS inhibits the enzymatic activities of recombinant target proteins *Pf*TIM, *Pf*GAPDH and *Pf*LDH. (G) Docking simulation of ATS binding to *Pf*LDH (PDB: 1T24) with −5.6 kcal/mol binding energy.

Declaration of competing interest

The authors declare that they have no known competing financial interests or personal relationships that could have appeared to influence the work reported in this paper.

Acknowledgments

The work was supported by grants from the National Key Research and Development Program of China (Nos. 2020YFA0908000 and 2022YFC2303600); the Innovation Team and Talents Cultivation Program of National Administration of Traditional Chinese Medicine (No. ZYYCXTD-C-202002); the National Natural Science Foundation of China (Nos. 82141001, 82274182, 82074098 and 82173914); the CACMS Innovation Fund (Nos. CI2021A05101 and CI2021A05104); the Scientific and Technological Innovation Project of China Academy of Chinese Medical Sciences (No. CI2021B014); the Science and Technology Foundation of Shenzhen (No. JCYJ20210324115800001); the Science and Technology Foundation of Shenzhen (Shenzhen Clinical Medical Research Center for Geriatric Diseases); Establishment of Sino-Austria "Belt and Road" Joint Laboratory on Traditional Chinese Medicine for Severe Infectious Diseases and Joint Research (No. 2020YFE0205100); the Fundamental Research Funds for the Central Public Welfare Research Institutes (Nos. ZZ14-YQ-050, ZZ14-YQ-051, ZZ14-YQ-052, ZZ14-FL-002, ZZ14-ND-010 and ZZ15-ND-10); Introduce innovative team projects of Jinan (No. 202228029); Shenzhen Governmental Sustainable Development Fund (No. KCXFZ20201221173612034); Shenzhen Key Laboratory of Kidney Diseases (No. ZDSYS201504301616234); Shenzhen Fund for Guangdong Provincial High-level Clinical Key Specialties (No. SZGSP001).

Supplementary materials

Supplementary material associated with this article can be found, in the online version, at doi:10.1016/j.cclet.2023.108296.

References

[1] World Health Organization. Available at: https://www.who.int/publications/i/item/9789240064898, 2022. (Accessed December 8, 2022).
[2] E.A. Ashley, M. Dhorda, R.M. Fairhurst, et al., N. Engl. J. Med. 371 (2014) 411–423.
[3] D. Menard, A. Dondorp, Cold Spring Harb, Perspect. Med. 7 (2017) a025619.
[4] J. Yang, Y. He, Y. Li, et al., Pharmacol. Ther. 216 (2020) 107697.
[5] J. Wang, C.J. Zhang, W.N. Chia, et al., Nat. Commun. 6 (2015) 10111.
[6] S. Krishna, A.C. Uhlemann, R.K. Haynes, Drug Resist. Updat. 7 (2004) 233–244.
[7] K.J. Wicht, S. Mok, D.A. Fidock, Annu. Rev. Microbiol. 74 (2020) 431–454.
[8] W. Asawamahasakda, I. Ittarat, Y.M. Pu, et al., Antimicrob. Agents Chemother. 38 (1994) 1854–1858.
[9] A. Robert, B. Meunier, et al., J. Am. Chem. Soc. 119 (1997) 5968–5969.
[10] B. Meunier, A. Robert, Acc. Chem. Res. 43 (2010) 1444–1451.
[11] H.M. Ismail, V. Barton, M. Phanchana, et al., Proc. Natl. Acad. Sci. U. S. A. 113 (2016) 2080–2085.
[12] H.M. Ismail, V.E. Barton, M. Panchana, et al., Angew. Chem. Int. Ed. 55 (2016) 6401–6405.
[13] S. Slavkovic, A.A. Shoara, Z.R. Churcher, et al., Sci. Rep. 12 (2022) 133.
[14] L.E. Heller, P.D. Roepe, Trop. Med. Infect. Dis. 4 (2019) 89.
[15] A. Mbengue, S. Bhattacharjee, T. Pandharkar, et al., Nature 520 (2015) 683–687.
[16] M.P. Gotsbacher, S.M. Cho, N.H. Kim, et al., ACS Chem. Biol. 14 (2019) 636–643.
[17] J. Li, T. Casteels, T. Frogne, et al., Cell 168 (2017) 86–100 e115.
[18] A.S. Lubin, A. Rueda-Zubiaurre, H. Matthews, et al., ACS Infect. Dis. 4 (2018) 523–530.
[19] P. Gao, Y.Q. Liu, W. Xiao, et al., Mil. Med. Res. 9 (2022) 30.
[20] W. Lei, F. Shen, N. Chang, et al., Chin. Chem. Lett. 32 (2021) 190–193.
[21] Z. Li, P. Hao, L. Li, et al., Angew. Chem. Int. Ed. 52 (2013) 8551–8556.
[22] T. Wang, Y. Zhou, H. Zheng, et al., Chin. Chem. Lett. 34 (2023) 107887.
[23] P.A. Stocks, P.G. Bray, V.E. Barton, et al., Angew. Chem. Int. Ed. 46 (2007) 6278–6283.
[24] J.E. Salcedo-Sora, E. Caamano-Gutierrez, S.A. Ward, et al., Trends. Parasitol. 30 (2014) 170–175.
[25] S. Saxena, L. Durgam, L. Guruprasad, J. Biomol. Struct. Dyn. 37 (2019) 1783–1799.
[26] D.L. Vander Jagt, L.A. Hunsaker, N.M. Campos, et al., Mol. Biochem. Parasitol. 42 (1990) 277–284.
[27] W.M. Brown, C.A. Yowell, A. Hoard, et al., Biochemistry 43 (2004) 6219–6229.
[28] S.S. Velanker, S.S. Ray, R.S. Gokhale, et al., Structure 5 (1997) 751–761.
[29] K. Ritter, A. Kuhlencord, R. Thomssen, et al., Lancet 342 (1993) 1333–1334.
[30] J.F. Satchell, R.L. Malby, C.S. Luo, et al., Acta Crystallogr. D: Biol. Crystallogr. 61 (2005) 1213–1221.
[31] S. Yerlikaya, E.D.A. Owusu, A. Frimpong, et al., Clin. Infect. Dis. 74 (2022) 40–51.
[32] C.A. Daubenberger, F. Pöltl-Frank, G. Jiang, et al., Gene 246 (2000) 255–264.